

000 BEYOND MEMORIZATION: 001 002 EXTENDING REASONING DEPTH WITH RECURRENCE, 003 004 MEMORY AND TEST-TIME COMPUTE SCALING

006 **Anonymous authors**

007 Paper under double-blind review

011 ABSTRACT

013 Reasoning is a core capability of large language models, yet how multi-step rea-
014 soning is learned and executed remains unclear. We study this in a controlled
015 cellular-automata (1dCA) framework that excludes memorisation by using disjoint
016 train/test rules. Models are trained on short state sequences, required to *infer* the
017 hidden local rule, and then *chain* it for multiple future steps. We find that most neu-
018 ral architectures learn the rule and achieve high next-step accuracy, but performance
019 drops sharply as the required number of steps increases. Increasing model depth is
020 crucial, and extending *effective* depth via recurrence, memory, or test-time compute
021 improves results but remains bounded. Complementing these controlled experi-
022 ments, a natural-language proxy game shows that contemporary LLMs largely fail
023 on the complex setting. Together, these results separate genuine rule induction from
024 memorisation, quantify how difficulty scales with reasoning depth, and highlight
025 the joint roles of architecture and training/inference procedures.

026 1 INTRODUCTION

028 Large Language Models (LLMs) demonstrate impressive capabilities in problem-solving and reason-
029 ing tasks, e.g., OpenAI’s o1 (OpenAI, 2024) and DeepSeek R1 (Guo et al., 2025) models achieved
030 a top-500 ranking in a qualifier for the USA Math Olympiad (AIME). OpenAI system achieved
031 an outstanding result, ranked 6 in the International Olympiad in Informatics (IOI 2025) (OpenAI,
032 2025). Both Google DeepMind and OpenAI systems achieve gold-medal scores in the International
033 Olympiad in Mathematics (IMO 2025) (Luong & Lockhart, 2025). On the other hand, extensive
034 evidence from ongoing research shows that LLMs still face challenges in multi-step reasoning Dziri
035 et al. (2024); Wan et al. (2024); Holliday & Mandelkern (2024); Gandarela et al. (2024); Mondorf &
036 Plank (2024); Shojaee et al. (2025) and planning Valmeekam et al. (2024), particularly when required
037 to infer and apply underlying rules from data.

038 These observations raise the following questions:

- 039 1. *Is the reasoning exhibited by LLMs the result of genuine generalization, or merely memorization?*
- 040 2. *How does task difficulty scale as the required number of reasoning steps increases?*
- 041 3. *To what extent do a model’s architectural inductive biases, training objectives, and inference*
042 *procedures limit its reasoning capabilities?*

043 Transformers (Vaswani et al., 2017) are universal function approximators and, with unbounded depth
044 and precision, are Turing-complete (Cybenko, 1989; Hornik et al., 1989; Dehghani et al., 2019; Yun
045 et al., 2019; Bhattacharya et al., 2020; Pérez et al., 2021; Sanford et al., 2024b). Yet, *finite-depth,*
046 *fixed-width* models used in practice cannot process arbitrarily long inputs in a single forward pass,
047 and they provably fail on tasks such as graph connectivity, Boolean formula evaluation, and exact
048 arithmetic beyond a bounded length (Merrill et al., 2022; Merrill & Sabharwal, 2023b; Strobl et al.,
049 2023; Feng et al., 2024).

050 One way to sidestep this depth barrier is to let the model *write its own scratch-pad* of intermediate
051 tokens. Chain-of-Thought (CoT) prompting, process supervision, and reinforcement learning (RL)
052 encourage models to emit multi-step rationales before producing the final answer (Wei et al., 2022;
053 Uesato et al., 2022; Wang et al., 2024; Yao et al., 2024; Kumar et al., 2024). Generating and
054 consuming these extra tokens effectively increases the computational depth in proportion to the

rationale length, enabling transformers to solve dynamic-programming benchmarks (Feng et al., 2024) and to recognize regular languages with linear decoding depth (Merrill & Sabharwal, 2023a). Yet, the main drawback is the need for supervision over intermediate steps, which is expensive or might be unavailable.

A complementary avenue is to *recycle hidden states*. Segment-level recurrence in memory-augmented transformers (Weston et al., 2015; Graves et al., 2014) enables the re-feeding of hidden states across segments (Dai et al., 2019; Rae et al., 2019; Bulatov et al., 2022; Chevalier et al., 2023; Rodkin et al., 2024), whereas state-space models achieve long-range interactions by leveraging linear dynamical systems (Gu et al., 2021; Gu & Dao, 2023). Recurrence deepens the network without emitting extra tokens, but the maximum number of recurrent steps is still limited by the input length. *Adaptive Computation Time* (ACT) (Graves, 2016) removes this upper bound entirely: the model learns to allocate a variable number of layer updates to each token, halting once further computation is predicted to be unhelpful. In principle, ACT grants transformers *unbounded effective depth* while preserving parameter efficiency, which is an appealing property for reasoning tasks that require widely varying amounts of computation.

In this paper, we study *rule abstraction* and *multi-step reasoning* in neural models using a controlled 1D Cellular Automata (1dCA) setting that prevents memorisation by holding out disjoint rule sets between training and test. We cast reasoning as variable-horizon prediction and quantify how architectures and depth-extension strategies cope as the look-ahead k increases. Our main contributions are:

1dCA-REASONING benchmark. A variable-length dataset with four task variants (O-S, O-O, O-RS, RO-S) that disentangle rule induction from state propagation; train/test rule sets are disjoint to preclude memorisation.

LLM evaluation in natural language. A new *Handsup* task—a worded proxy equivalent to the 1dCA update—used to assess LLMs under varying look-ahead and rule complexity, showing that many LLMs (except Gemini 2.5 Pro) fail on the simplest radius-1 setting.

Comprehensive architectural comparison. Side-by-side evaluation of Transformers (GPT-NeoX), LSTMs, state-space models (Mamba), and a memory-augmented Transformer (ARMT) under identical conditions. Fixed-depth (4-layer) models solve $k=1$ but collapse for $k \geq 2$; ARMT extends to $k=2$. We corroborate these trends on a group-multiplication benchmark (Merrill et al., 2024).

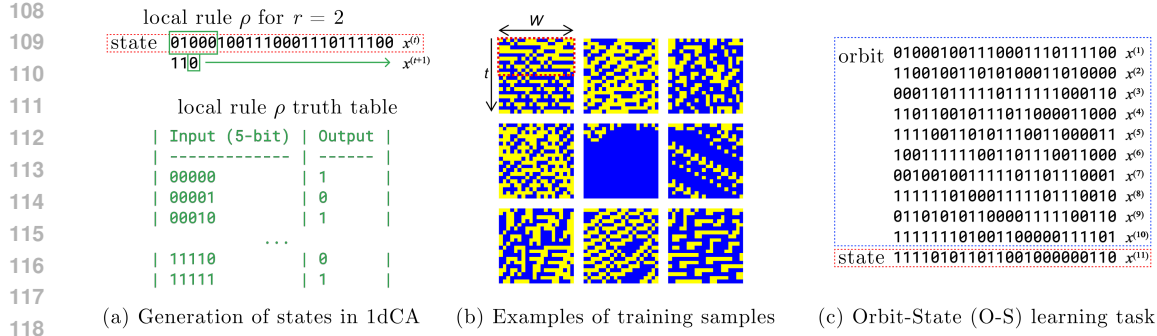
Depth-extension analysis. With 4-layer backbones: (i) Adaptive Computation Time (ACT) reliably adds $\sim +1$ effective step with modest compute; (ii) GRPO (RL) reaches $k=3$ *without* intermediate supervision; and (iii) token-level Chain-of-Thought attains near-perfect accuracy up to $k=4$.

2 METHODS

Modeling Reasoning with 1d Cellular Automata. Reason is the capacity of consciously applying logic by drawing valid conclusions from new or existing information.¹ Reasoning about an unfamiliar process naturally splits into two parts: (i) inferring the hidden law that drives state transitions and (ii) chaining that law to predict multiple future steps. One-dimensional cellular automata (1dCA) provide a minimal, fully observable sandbox for this: a local Boolean rule—the toy universe’s “micro-physics”—updates each binary state from its neighborhood. In our benchmark the rule is withheld and the train/test rule sets are disjoint, so rote lookup cannot succeed. To solve a task the model must first induce the rule from observed orbits and then apply it repeatedly to roll out future states, cleanly separating genuine rule-based reasoning from mere memorization.

Background. An *One-dimensional Cellular Automaton* (1dCA) is a one-dimensional, dynamical system in which space and time are discrete. Let $r \in \mathbb{N} : r \geq 1$ be the *neighborhood radius* in the space represented by a regular lattice of $W \in \mathbb{N} : W \geq 2r + 1$ identical, locally-interconnected *cells* with binary state spaces, $\mathbb{S} = \{0, 1\}$. The 1dCA’s *global state*, $x \in \mathbb{S}^W$, is a lattice configuration specified by the values of all states of all cells in the lattice at a given time. This state evolves deterministically in synchronous, discrete time steps according to a *global map* $g_\rho : \mathbb{S}^W \rightarrow \mathbb{S}^W$ defined by a *local rule* $\rho : \mathbb{S}^{2r+1} \rightarrow \mathbb{S}$, so $[g_\rho(x)]_w = \rho(x_{w-r}, \dots, x_w, \dots, x_{w+r})$ (Fig.1a). The sequence of states an 1dCA passes through during its *space-time evolution*, $\mathcal{O}^T(x) = [x, g_\rho(x), g_\rho(g_\rho(x)), \dots, g_\rho^{oT-1}(x)]$,

¹<https://en.wikipedia.org/wiki/Reason>



119 **Figure 1: Learning One-dimensional Cellular Automata.** (a) Update of state with local rule.
120 (b) Orbit of 1dCA is a sequence of binary strings of size $W = 20$. The first $k = 10$ states marked by
121 the red rectangle encode transformer input. (c) Given a part of the orbit a model learns to predict the
122 next state (O-S).
123
124

125 defines its *trajectory* or *orbit* from an *initial condition* (configuration) x for $T \in \mathbb{N} : T \geq 1$. Examples
126 of 1dCA orbits are visualized in Figure 1(b).
127

128 **Benchmark for reasoning.** Our benchmark instantiates multi-step reasoning with 1dCA trajectories:
129 each example provides a short orbit (e.g., 10 states) generated by a hidden rule; training and test
130 use disjoint rule sets. The model must infer the rule from the observed states and predict future
131 configurations, forcing it to learn a general rule-inference procedure rather than memorize instance-
132 specific mappings. We vary difficulty via *look-ahead* prediction: to give $g_\rho^{oT+k}(x)$ for $k \in \{1, 2, 3, 4\}$
133 steps ahead (without intermediate states), the model must internally roll out the dynamics, effectively
134 chaining the inferred rule. We call k the *depth of reasoning* and study which architectures can achieve
135 greater depth under this setting.
136

137 **Task variants.** The benchmark could emulate the situations when we have supervision on intermediate
138 steps (i.e. the thinking process of the LLM) and when we only have a final look-ahead state. We
139 consider four variations of learning tasks designed to assess different aspects of predictive modeling
140 and rule inference:
141

142 **Orbit-State (O-S):** given an orbit $\mathcal{O}^T(x) = [x^{(1)}, x^{(2)}, \dots, x^{(T)}]$ where $x^{(1)} \in \mathbb{S}^W$, the objective
143 is to predict the state $x^{(T+k)}$ at look-ahead $k \in \mathbb{N} : k \geq 1$. For $k = 1$ (see Fig.1c) this is a
144 single-step prediction simulating an elementary act of reasoning or a part of a curriculum to learn
145 longer reasoning chain. For $k > 1$ multiple intermediate inference steps are required for the answer.
146

147 **Orbit-Orbit (O-O):** given an orbit $\mathcal{O}^T(x)$ for some $k > 1$ predict the subsequent states up to time
148 $T + k$, generating $\mathcal{O}_{T+1}^{T+k}(x) = [x^{(T+1)}, \dots, x^{(T+k)}]$. This task simulates step-by-step multi-step
149 reasoning as a learning objective.
150

151 **Orbit-State and Rule (O-RS):** given an orbit $\mathcal{O}^T(x)$ predict the state $x^{(T+k)}$ and the local rule ρ . By
152 explicitly optimizing rule prediction, the model receives direct supervision.
153

154 **Rule and Orbit-State (RO-S):** given an orbit $\mathcal{O}^T(x)$ and the local rule ρ predict the state $x^{(T+k)}$ at
155 time $T + k$. Since the rule is explicitly provided, the model can bypass inference of rule structure
156 and focus solely on learning to apply the update.
157

158 The rule in our 1dCA setup is based on a neighborhood radius $r = 2$, meaning each bit of the next
159 state depends on a 5-bit window (2 left + current cell + 2 right) from the current state. Since there
160 are 2^5 possible 5-bit strings, the rule mapping can be represented by a 32-bit string. Each bit in this
161 string corresponds to the output of the rule for a specific input. The position of this output bit within
162 the rule string is determined by the binary value of the 5-bit input (see Fig.1a). For our evaluation we
163 use the exact match metric for state prediction (1 if the state is predicted correctly, 0 if at least one bit
164 is predicted wrong) and bit accuracy (ratio of the correctly predicted bits) for the rule. You can find
165 the examples of training/validation samples in the subsection F.2.
166

167 **Neural Models.** In our study, we consider LLMs and small models belonging to several widely-
168 applied architectural families. Long Short-Term Memory (LSTM) networks Hochreiter & Schmidhu-

ber (1997), a class of recurrent neural network (RNN), have proven effective in capturing sequential dependencies in NLP tasks. However, their inherent sequential processing limits efficiency and scalability. Transformers Vaswani et al. (2017) address these limitations by processing entire input sequences simultaneously through self-attention, enabling parallel computation and better handling of long-range dependencies compared to RNN-based models. State space models (SSMs) Gu et al. (2021) offer an alternative approach to sequence modeling by leveraging structured state representations and computationally efficient recurrence mechanisms. We consider the Associative Recurrent Memory Transformer (ARMT) Rodkin et al. (2024), an extension of the transformer designed to enhance memory capabilities. ARMT builds on the Recurrent Memory Transformer Bulatov et al. (2022) by incorporating quasi-linear attention mechanisms that improve information transfer across input blocks, mitigating limitations in long-context processing. We discuss the properties of these models in Appendix C.

We also explore several approaches for enhancing reasoning in neural networks, such as Chain-of-Thought, RL-methods (GRPO), and Adaptive Computations Time.

Chain-of-Thought (CoT), prompting Wei et al. (2022) is a technique for enhancing the reasoning capabilities of LLMs. Unlike standard prompting techniques, which attempt to directly infer an answer from the input, CoT forces the model to explicitly generate intermediate reasoning steps while solving a problem, allowing it to reference these tokens as a form of recurrent state. This mechanism effectively increases the formal computational power of the model Merrill & Sabharwal (2023a) and extends its effective depth enabling LLMs to perform multi-step reasoning, particularly in tasks such as mathematical problem-solving, logical inference, and commonsense reasoning Wei et al. (2022).

Learning to reason with RL. Another common practice involves training LLMs with reinforcement learning methods such as proximal policy optimization (PPO) Schulman et al. (2017) and group relative policy optimization (GRPO) Shao et al. (2024) after supervised finetuning in order to improve the generation of reasoning traces. RL post-training has been shown to improve instruction following Ouyang et al. (2022) as well as mathematical Wang et al. (2024) and general reasoning performance in LLMs Havrilla et al. (2024); Kumar et al. (2024); Guo et al. (2025). Compared to supervised methods, training to reason with GRPO requires no supervision on intermediate reasoning steps. It only relies on rewards from correct final answers and maintaining the desired format.

Adaptive Computation Time (ACT). (Graves, 2016) is the mechanism proposed to allow recurrent and self-attentive models to perform a variable number of computation steps within each time-step dynamically. The core idea is to enable different parts of the sequence to have different computational complexities, which is particularly useful for tasks with non-uniform requirements for computation. In this class of models a halting unit dynamically decides how much “thinking time” should take place at each step, thus adaptively scaling the effective reasoning depth of the model. For mathematical formulation check the Appendix E.

Recurrent Memory Transformers. As a trade-off between expressive recurrent models and efficiently trainable transformers, the Recurrent Memory Transformer was proposed (Bulatov et al., 2022). It leverages recurrent steps between the fixed-sized segments, while the tokens inside these segments are processed in parallel with the transformer model, which RMT augments. In the original RMT (Bulatov et al., 2022), the recurrent steps are performed by passing the output of special memory tokens from one segment to the input of the next segment. In the enhanced version of RMT: Associative Recurrent Memory Transformer (Rodkin et al., 2024), the recurrent steps are performed with quasi-linear attention in each transformer layer. In this work, we use the ARMT as a representative of recurrent memory transformers.

3 EXPERIMENTS

We start our study with testing contemporary LLMs on a commonsense, natural-language task that is *formally equivalent* to our 1D cellular automata (1dCA) setup. The goal is to assess how well current models can (i) infer a simple logic rule from observations and (ii) chain that rule for multiple steps.

LLMs performance on the *Handsup* game. A group of friends sits around a table. In each round n , every friend i has a binary state: `up` (hand raised) or `down`. The hidden rule has radius $r \in \{1, 2\}$: the state of friend i at round n depends only on the $(2r+1)$ -tuple $\{i-r, \dots, i, \dots, i+r\}$ from round

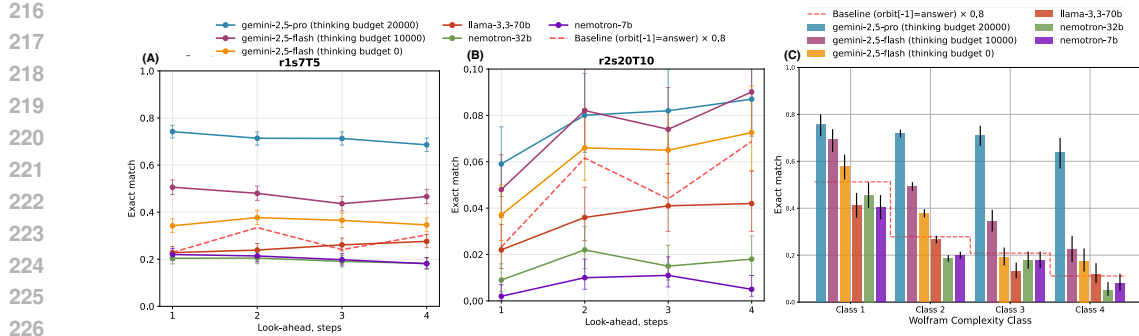


Figure 2: **Large Language Models struggle to solve reasoning 1dCA style tasks in natural language game.** (a) Only Gemini-2.5-pro sustainably achieves high scores in predicting the next state in Handsup game with $r=1$ and $w=7$ players given history of $T=5$ rounds. (b) None of models achieve reasonable performance (above 10%) for harder game with more distant dependencies ($r=2$), more friends (20) and longer history (10). Only Gemini models achieve scores higher than the *baseline* score, where the round is predicted the same as the last known round. (c) shows performance on the simple handsup game across different subsets of the dataset, split with respect to the Stephen Wolfram’s rule classification of ECA. We observe the performance degradation on the tasks with rules of higher complexity (Class 3 and 4). All values are mean exact match with 95% CIs. The final game state was extracted from the models’ answers with Gemma3-12B-IT model with $\approx 80\%$ EM extraction accuracy so we scale the baseline accordingly.

$n-1$. This is exactly an 1dCA-style local update $\rho : \{0, 1\}^{2r+1} \rightarrow \{0, 1\}$. We describe in natural language the first $N \in \{5, 10\}$ rounds and ask the model to predict the behaviour of players at round $N+s$ with $s \in \{1, 2, 3, 4\}$. We evaluate *exact-match* accuracy on the target round. To probe difficulty, we consider families of rules at $r=1$ and $r=2$, and for $r=1$ also group rules by Wolfram complexity class. We compare Gemini 2.5 Pro and Gemini 2.5 Flash with different “thinking budgets” (20k, 10k, and 0), Llama-3.3-70B, and Nemotron-32B/7B.

Figure 2 reports LLMs performance on Handsup game. In the simple game (fig. 2a) equivalent to elementary CA ($r=1, w=7, T=5, 256$ possible rules) only Gemini 2.5 Pro shows solid performance with a mild decline as look-ahead increases (about $0.72 \rightarrow 0.69$ from $s=1$ to $s=4$). Gemini 2.5 Flash performs lower with a thinking budget helps slightly over zero budget. Llama-3.3-70B and Nemotron 7B models hover around the trivial baseline across s . The hard game ($r=2, w=20, T=10, \approx 4.3B$ possible rules) represents a strong challenge to existing LLMs (see fig. 2b) as no model cross 10% EM with only Gemini models marginally over trivial baseline. As Fig. 2c shows accuracy decreases with dynamical complexity of the rule according to Wolfram’s complexity classes. Gemini 2.5 Pro is consistently best (roughly 0.75 in Class 1 down to ≈ 0.63 in Class 4), Flash trails Pro, and open-weight baselines lag below ≈ 0.4 in Classes 2–4. None of the models are uniformly robust across classes.

The *Handsup* results directly inform our research questions. The failure of most LLMs—even with “thinking” budgets—to solve the simplest radius-1 setting challenges the view that current successes reflect robust generalization rather than pattern recall (RQ1). Performance degrades systematically with more complex dependencies ($r=2$) and higher Wolfram classes, quantifying how difficulty scales with required reasoning steps (RQ2). Finally, to disentangle whether these failures stem from architectural limits versus training/inference procedures, we proceed to controlled small-model studies that test architectural capacity under matched supervision; success would implicate training as the bottleneck, while failure would argue for architectural changes (RQ3).

Single-step performance across neural architectures. We generated an 1dCA dataset with the CellPyLib Antunes (2021) for the fixed lattice size $W = 20$ and neighborhood radius $r = 2$. This configuration results in a total of $2^{2r+1} \approx 4.3 \times 10^9$ possible Boolean functions defining local rules. For each sample in the dataset, both the initial state and the local rule ρ were generated randomly. We then computed the orbit for $T = 20$ time steps using these parameters. The training dataset consists of 9.5×10^5 instances and the test of 10^5 instances. Importantly, the local rules included in the test set

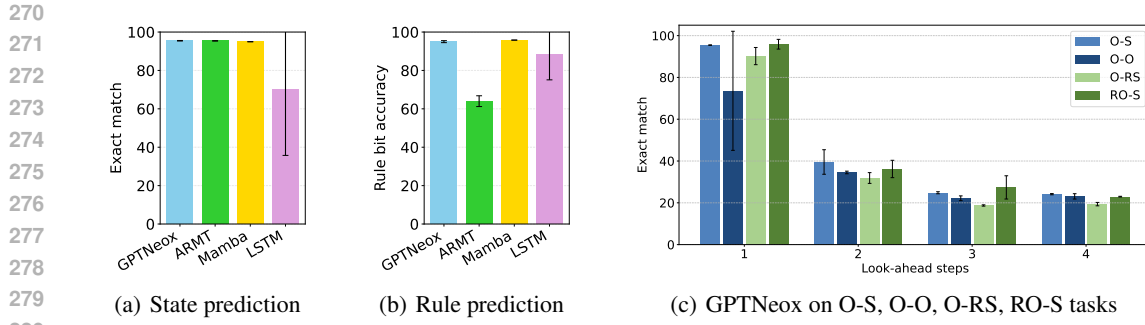


Figure 3: **Single-step accuracy is near-perfect across models, but multi-step performance collapses.** (a) Exact-match accuracy for single-step *state prediction* (O-S): all models except LSTM achieve >95 %. (b) Bit-wise accuracy for *rule inference* (O-RS): most architectures recover the hidden Boolean rule, yet ARMT trails the rest. (c) GPTNeox accuracy on variable-horizon prediction across the four task variants (O-S, O-O, O-RS, RO-S): accuracy falls steeply with look-ahead k .

are exclusive and not present in the training set. This separation ensures that the model’s performance reflects its ability to generalize to unseen rules, rather than simply memorizing the training data.

As shown in Figure 3(a), models with different architectures can predict one step forward with nearly perfect accuracy. LSTM performs slightly worse than other architectures, likely due to challenges in effectively encoding the binary state representation. Successful learning demonstrate that the Transformer model is capable of generalizing not only over initial conditions for a particular function — commonly the focus in studies of transformer trainability in CA domain — but also across different Boolean functions of fixed arity (5 in our case).

When tasked with predicting both future states and the underlying rules (O-SR setting), Figure 3(b) shows that models generally achieve high accuracy on rule prediction, though with interesting variations. ARMT notably struggles with accurate rule inference compared to other architectures, despite handling next-state prediction well.

Limitations in the Reasoning Depth of Transformers. We selected a 4-layer architecture with $d_{\text{model}}=128$ as a baseline configuration for our experiments. Using this configuration, we separately trained from scratch for each look-ahead step $k \in \{2, 3, 4\}$ of the O-S task the GPTNeox (Black et al., 2022) model to predict the state at time $x^{(T+k)}$ given an orbit $\mathcal{O}^T(x) = [x^{(1)}, x^{(2)}, \dots, x^{(T)}]$. As presented in Figure 3(c), this task proved to be challenging. While the average accuracy for next-state prediction (O-S task with $k=1$) was 0.95, it dropped to 0.40 for $k=2$ and fell below 0.25 for $k=3$ and $k=4$. Despite having four layers, which in principle could capture up to two or three sequential transformations if effectively utilized, the model still struggles to learn look-ahead tasks for $k \geq 2$. Specifically, the same model’s depth that suffices for the single-step O-S task is no longer adequate for maintaining accurate multi-step predictions, suggesting that the capacity is being taxed by the need to encode and apply repeated rule updates in a fixed number of transformations.

To determine whether this decline was due to the GPTNeox’s architecture or the training objective, we explored whether accuracy could be improved by training the model to predict intermediate steps. This approach is analogous to multi-token prediction (Gloockle et al., 2024). We employed the Orbit-Orbit (O-O) task, training the model to predict the next four states in parallel. The results, also shown in Figure 3(c), indicate that the model’s predictive abilities degrade in this training scenario, as even prediction of the next state ($k=1$) is less than 0.80 accuracy. However, the higher standard deviation suggests that it happens because of the instability of such training: some runs could simply fail, while others could work well (as shown by the exact match of $k=2, 3, 4$ being relatively close to the O-S scenario).

These results suggest that learning to store a hidden representation of intermediate states (as in the O-S, O-RS and RO-S with $k > 1$) is hard for the model. Surprisingly, a direct supervision for a hidden representation of the underlying rule (O-RS) is more challenging initially and does not facilitate better generalization to longer planning horizons. This implies that explicitly encouraging

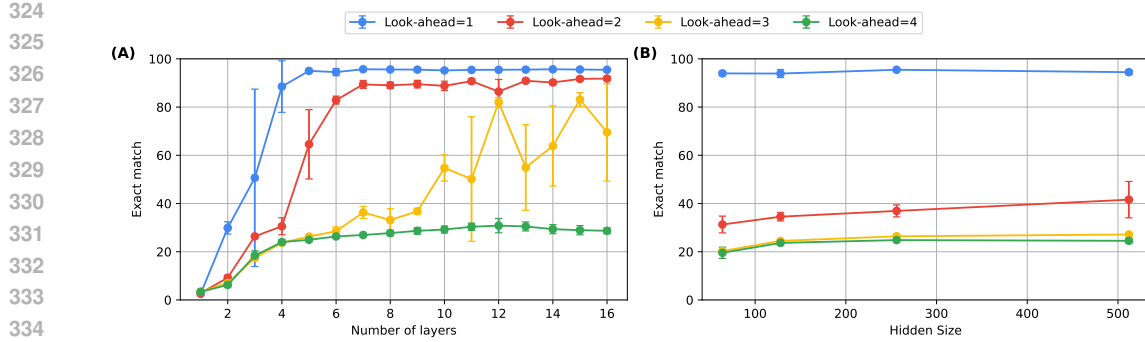


Figure 4: **Depth — not width — drives multi-step accuracy.** Exact-match accuracy for look-ahead horizons $k \in \{1, 2, 3, 4\}$ as a function of (a) transformer layer count and (b) embedding dimension d_{model} . Deeper networks boost performance sharply for $k \geq 2$ and plateau beyond six layers, whereas widening the model yields only marginal gains across all horizons.

the model to infer the generating rule cannot enhance its ability to make longer-term predictions by reinforcing the internalization of the system’s dynamics.

Finally, we explored the scenario where the local rule ρ is explicitly provided to the model, corresponding to the Rule and Orbit-State (RO-S) task. Intuitively, this should be the easiest task for the model, as it eliminates the need to infer the rule from the orbit. As shown in Figure 3(c), GPTNeox indeed learns to apply the given rule for next-state prediction with near-perfect accuracy for $k = 1$. Surprisingly, however, the performance for look-ahead steps $k = 2, 3$ and 4 drops to the level of original O-S predictions. The poor performance on look-ahead steps $k > 1$ raises the question of whether this limitation stems from the neural network’s parameter count, layer width, or width of its embeddings. To answer this question, we performed the experiments, while varying the number of transformer layers and the embedding dimension d_{model} .

Figure 4 (a) shows that accuracy for one- and two-step prediction saturates after 4–6 layers. Three-step prediction, however, continues to improve up to about 12 layers, whereas four-step prediction remains poor regardless of depth. Figure 4 (b) examines width. Increasing d_{model} provides only marginal gains across all horizons, with the most noticeable bump occurring between 64 and 128 dimensions; further widening yields diminishing returns. These results illustrate the importance of increasing the model’s depth rather than the width of its embeddings for better multi-step reasoning performance.

Extending the depth of reasoning with Adaptive Computation Time. The previous subsection confirmed that simply *adding layers* offers a clear performance boost, yet even a 12-layer transformer still falters for $k \geq 4$ (Fig. 4a). Here, we set the depth to 4 layers and study if it’s possible to improve performance by techniques that expand a model’s *effective* depth at inference time—segment-level recurrence and *Adaptive Computation Time* (ACT). Hyperparameters for all models can be found in Table 1. Both approaches inject extra computational steps without further increasing the static layer count, potentially enabling deeper reasoning while preserving parameter efficiency.

Figure 5 (A) shows that the auto-regressive models – GPTNeox, LSTM, and Mamba ² – handle next-state prediction but fail to solve the multi-step task. Only ARMT manages to extend its capacity up to two look-ahead steps, likely because it processes sequences segment by segment and is thus forced to separate rule and state representations. This separation may enable the generation of a hidden representation for the intermediate state, followed by the application of the rule, effectively enhancing the depth of the model reasoning.

Augmenting models with ACT has little effect on all architectures except GPTNeox, which sees improved performance at $k = 2$ but not at $k = 3, 4$. Overall, ARMT makes effective use of

²We use the architecture from the previous section: 4 layer GPTNeox with $d_{\text{model}} = 128$ and 4 attention heads. For Mamba, we use a state size of 16. For ARMT, $d_{\text{mem}} = 32$. As ARMT is a segment-level model, we segment our state sequence in the way that each segment contains a pair of consecutive states in the orbit, and the prediction is performed in the last segment with the last CA state from the input in it. We report average results of 3 models trained with different seeds.

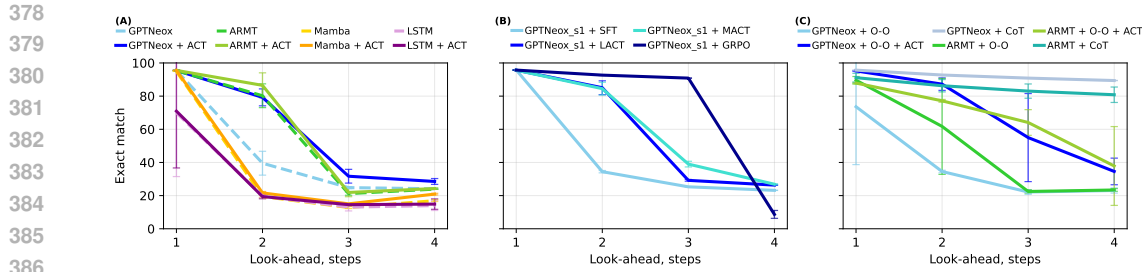


Figure 5: **Extensions of computation depth enhance the reasoning abilities of transformer-based models.** Values are exact match of the $x^{(T+k)}$ state prediction for look-ahead steps $k \in \{1, 2, 3, 4\}$. **(a)** ACT significantly improves computational abilities of transformer-based models in multi-step prediction. **(b)** Without supervision on intermediate reasoning steps RL training with GRPO allows the model to extrapolate reasoning on 3 steps forward. **(c)** With step-by-step supervision, the CoT approach significantly outperforms the in-depth approach of ACT. GPTNeox and ARMT with both ACT and O-O supervision perform the best.

the transformer’s four-layer depth but cannot extend beyond it. Likewise, while ACT helps the transformer make use of its existing layers more efficiently, it fails to enable any architecture to solve three- or four-step predictions. Moreover, LSTM and Mamba are unable to master multi-step tasks with or without ACT, likely due to representation bottlenecks in their hidden states.

We subsequently chose to train GPTNeox model that is already capable of performing one-step reasoning with the SFT, LACT, MACT, and GRPO methods, with the goal of enabling it to reason over multiple steps without access to supervision for the intermediate reasoning stages. As illustrated in Figure 5 (B), standard supervised fine-tuning (SFT) fails to address the problem effectively. Although the model is primarily trained on a one-step prediction task, it struggles to apply the rule iteratively. Consistent with previous results (Fig. 5 (A)), applying ACT both at the layer level (LACT) and across the entire model (MACT) improves performance on the two-step prediction task but does not generalize beyond that. Interestingly, when trained using RL (GRPO) and granted the capability to autoregressively generate intermediate “thinking” tokens before producing the final output, the model succeeds on the three-step prediction task. The reward signal is defined as the average token-level accuracy of the model’s prediction following the end-of-thinking token.

Reasoning Supervision. We examine the impact of reasoning supervision on GPTNeox and ARMT, along with their corresponding ACT-augmented variants. To this end, we replicate the O-O training setup by incorporating mask tokens into the autoregressive models within a causal masking framework. Figure 5 (C) shows that contrary to our expectations, the O-O training objective alone does not yield performance improvements for either GPTNeox or ARMT. However, the integration of O-O training with ACT results in superior performance, surpassing both the baseline and ACT-only variants.

As a final step, we combined GPTNeox and ARMT with a token-by-token CoT-like next-token prediction training. Under this regime, both models succeed at multi-step prediction up to $k = 4$, with GPTNeox slightly outperforming ARMT across each look-ahead distance (Fig. 5 (C)). These results suggest that, when explicit reasoning supervision is available, a chain-of-thought-inspired approach to training offers a particularly effective strategy for enabling multi-step reasoning.

In addition to the cellular automata experiments, in Appendix H we show the significance of our findings on group multiplication benchmark (Merrill et al., 2024).

4 DISCUSSION AND CONCLUSIONS

Our study examines how *architecture*, *training signal*, and *depth-extension strategy* jointly determine a model’s ability to learn multi-step reasoning in 1dCA—*without memorization*, since train/test rules are disjoint. The headline results (aggregated in Appendix A, Figure 6) speak directly to our research questions **RQ1–RQ3**.

- **Models can infer unseen rules, but LLMs falter on the simplest case (RQ1).** Both Transformers and recurrent/SSM variants (GPT-NeoX, LSTM, Mamba, ARMT) succeed on rule induction from orbits—evidence of genuine generalization because evaluation uses unseen rules. However, evaluated LLMs (except Gemini 2.5 Pro) fail to reliably solve even the radius-1 *Handsup* setting, indicating that scale and generic “think more” prompting are insufficient.
- **Reasoning difficulty grows sharply with look-ahead depth (RQ2).** Fixed-depth (4-layer) models $k=1$ but collapse for $k \geq 2$, revealing a clear depth barrier.
- **Adaptive halting adds $\approx +1$ effective step at low compute cost (RQ3).** Adding Adaptive Computation Time (ACT) to a Transformer consistently shifts the depth frontier (roughly $k:1 \rightarrow 2$ or $2 \rightarrow 3$) without increasing parameters, with diminishing returns past $k \approx 3$.
- **GRPO reaches three-step rollouts without intermediate supervision (RQ3).** RL rewarding final correctness only matches CoT@ $k=2$ performance at $k=3$.
- **Token-level CoT saturates the current benchmark up to four steps (RQ3).** With stepwise targets, GPT-NeoX attains $> 99\%$ accuracy for $k \leq 4$ (Figure 5C), showing that explicit supervision can elicit deeper computation given availability of intermediate labels.
- **Depth limits align with capacity constraints and can be partially mitigated (RQ2/RQ3).** Models with shallow effective depth (e.g., TC⁰-like limitations) require more layers to track longer computations; ACT partially alleviates this on harder state-tracking (e.g., group-multiplication) tasks but does not fully resolve the gap.

Broader implications for LLM reasoning—and beyond. Our results align with a growing body of evidence that *reasoning failures often stem from insufficient depth allocation and sparse optimisation signals*. For LLMs, this suggests that (i) **prompt engineering alone is unlikely to improve multi-step reasoning**: unless intermediate steps are reinforced—via CoT, search-augmented decoding, or RL-style self-critique—models tend to default to shallow heuristics; (ii) **adaptive-depth mechanisms are a promising scaling direction**: ACT-style halting, deployed token-wise or layer-wise, can allocate computation on demand to match the variable complexity of real queries; and (iii) **explicit intermediate representations remain the most reliable route** to multi-step generalisation via CoT.

Beyond language, the same principles apply to neural algorithmic reasoning, robotic planning, and scientific simulation: whenever the target task contains latent iterative structure, giving the network *room*—via dynamic recurrence, learned halting, or supervised scratch-pads—to run the hidden algorithm is more data-efficient than brute-force depth. We therefore advocate future benchmarks that (a) separate rule induction from state propagation, (b) report *effective depth* alongside accuracy, and (c) evaluate adaptive-computation policies explicitly. Progress along these axes will benefit not only next-generation LLMs but also neural systems tasked with symbolic manipulation, formal verification, and open-ended planning.

Conclusions. We introduced 1dCA reasoning benchmark that isolates multi-step reasoning *without memorisation* by using disjoint train/test rule sets. Success therefore reflects genuine *rule inference* followed by iterative application, not lookup.

Empirically, fixed-depth (4-layer) models—Transformers, LSTMs, and state-space models—show a sharp depth cutoff: they solve $k=1$ but collapse for $k \geq 2$. Segment-recurrent attention (ARMT) extends this to $k=2$ yet remains bounded. Adding Adaptive Computation Time (ACT) provides a compute-efficient $\sim +1$ effective step (with diminishing returns beyond $k \approx 3$). Reinforcement learning via GRPO achieves reliable $k=3$ *without* intermediate labels, while token-level Chain-of-Thought attains near-perfect accuracy up to $k=4$. Complementing these small-model results, most contemporary LLMs—*except* Gemini 2.5 Pro—struggle even on the simplest natural-language proxy (radius-1 *Handsup*), underscoring that scale and generic “think more” prompting are insufficient.

Together, these findings support our contributions: (1) a benchmark that cleanly separates rule induction from state propagation; (2) a systematic architectural comparison; (3) an analysis of depth-extension mechanisms (recurrence, halting, RL, and explicit stepwise supervision); and (4) practical guidance on eliciting deeper computation. More broadly, they show that *how* we train and allocate compute can matter as much as *what* we train: objectives that force multi-step prediction and mechanisms that adaptively allocate depth are decisive, while explicit intermediate representations remain the most reliable route to deeper generalisation.

486
487

LIMITATIONS

488
489
490
491

While our findings offer valuable insights into methods for enhancing reasoning, we acknowledge that the study is limited to small-scale models, and certain conclusions may not generalize directly to large language models. Our LLM evaluation covers only selected models over the main classes and sizes.

492

493
494

REPRODUCIBILITY STATEMENT

495
496
497
498
499

Metrics are reported with 95% confidence intervals for handsup game with language models. In all small models finetuning experiments we report standard deviation estimates (square root of unbiased variance estimation) for confidence intervals. All hyperparameters are specified in Table 1, and we describe training details and used hardware in Section D. We also release the full codebase to ensure reproducibility of results: https://anonymous.4open.science/r/beyond_memorization.

500

501
502

REFERENCES

503
504
505

Luis M. Antunes. Cellpylib: A python library for working with cellular automata. *Journal of Open Source Software*, 6(67):3608, 2021. doi: 10.21105/joss.03608. URL <https://doi.org/10.21105/joss.03608>.

506
507
508

Satwik Bhattacharya, Arkil Patel, and Navin Goyal. On the computational power of transformers and its implications in sequence modeling. *arXiv preprint arXiv:2006.09286*, 2020.

509
510
511
512
513

Sid Black, Stella Biderman, Eric Hallahan, Quentin Anthony, Leo Gao, Laurence Golding, Horace He, Connor Leahy, Kyle McDonell, Jason Phang, Michael Pieler, USVSN Sai Prashanth, Shivanshu Purohit, Laria Reynolds, Jonathan Tow, Ben Wang, and Samuel Weinbach. Gpt-neox-20b: An open-source autoregressive language model, 2022. URL <https://arxiv.org/abs/2204.06745>.

514
515
516
517
518

Aydar Bulatov, Yury Kuratov, and Mikhail Burtsev. Recurrent memory transformer. In S. Koyejo, S. Mohamed, A. Agarwal, D. Belgrave, K. Cho, and A. Oh (eds.), *Advances in Neural Information Processing Systems*, volume 35, pp. 11079–11091. Curran Associates, Inc., 2022. URL https://proceedings.neurips.cc/paper_files/paper/2022/file/47e288629a6996a17ce50b90a056a0e1-Paper-Conference.pdf.

519
520
521

Alexis Chevalier, Alexander Wettig, Anirudh Ajith, and Danqi Chen. Adapting language models to compress contexts. *arXiv preprint arXiv:2305.14788*, 2023.

522
523

George Cybenko. Approximations by superpositions of a sigmoidal function. *Mathematics of Control, Signals and Systems*, 2:183–192, 1989.

524
525
526

Zihang Dai, Zhilin Yang, Yiming Yang, Jaime G Carbonell, Quoc Le, and Ruslan Salakhutdinov. Transformer-xl: Attentive language models beyond a fixed-length context. In *Proceedings of the 57th Annual Meeting of the Association for Computational Linguistics*, pp. 2978–2988, 2019.

527
528
529
530

Mostafa Dehghani, Stephan Gouws, Oriol Vinyals, Jakob Uszkoreit, and Lukasz Kaiser. Universal transformers. In *International Conference on Learning Representations*, 2019. URL <https://openreview.net/forum?id=HyzdRiR9Y7>.

531
532
533

Gregoire Deletang, Anian Ruoss, Jordi Grau-Moya, Tim Genewein, Li Kevin Wenliang, Elliot Catt, Chris Cundy, Marcus Hutter, Shane Legg, Joel Veness, et al. Neural networks and the chomsky hierarchy. In *The Eleventh International Conference on Learning Representations*, 2023.

534
535
536
537

Nouha Dziri, Ximing Lu, Melanie Sclar, Xiang Lorraine Li, Liwei Jiang, Bill Yuchen Lin, Sean Welleck, Peter West, Chandra Bhagavatula, Ronan Le Bras, et al. Faith and fate: Limits of transformers on compositionality. *Advances in Neural Information Processing Systems*, 36, 2024.

538
539

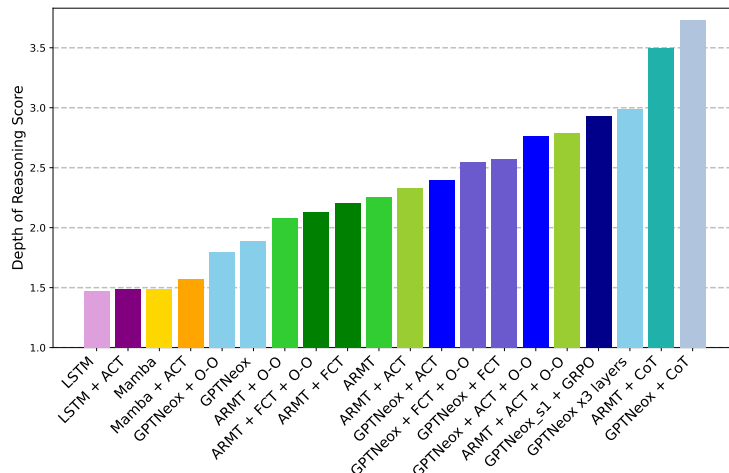
Guobao Feng, Bohang Zhang, Yuntian Gu, Haotian Ye, Di He, and Liwei Wang. Towards revealing the mystery behind chain of thought: a theoretical perspective. *Advances in Neural Information Processing Systems*, 36, 2024.

- 540 João Pedro Gandarela, Danilo S Carvalho, and André Freitas. Inductive learning of logical theories
 541 with llms: A complexity-graded analysis. *arXiv preprint arXiv:2408.16779*, 2024.
- 542
- 543 Fabian Gloeckle, Badr Youbi Idrissi, Baptiste Rozière, David Lopez-Paz, and Gabriel Synnaeve.
 544 Better & faster large language models via multi-token prediction. *arXiv preprint arXiv:2404.19737*,
 545 2024.
- 546
- 547 Sachin Goyal, Ziwei Ji, Ankit Singh Rawat, Aditya Krishna Menon, Sanjiv Kumar, and Vaishnavh
 548 Nagarajan. Think before you speak: Training language models with pause tokens. In *The Twelfth
 549 International Conference on Learning Representations*, 2024.
- 550
- 551 Alex Graves. Adaptive computation time for recurrent neural networks. *arXiv preprint
 552 arXiv:1603.08983*, 2016.
- 553
- 554 Alex Graves, Greg Wayne, and Ivo Danihelka. Neural turing machines. *arXiv preprint
 555 arXiv:1410.5401*, 2014.
- 556
- 557 Albert Gu and Tri Dao. Mamba: Linear-time sequence modeling with selective state spaces. *arXiv
 558 preprint arXiv:2312.00752*, 2023.
- 559
- 560 Albert Gu, Karan Goel, and Christopher Re. Efficiently modeling long sequences with structured
 561 state spaces. In *International Conference on Learning Representations*, 2021.
- 562
- 563 Daya Guo, Dejian Yang, Haowei Zhang, Junxiao Song, Ruoyu Zhang, Runxin Xu, Qihao Zhu,
 564 Shirong Ma, Peiyi Wang, Xiao Bi, et al. Deepseek-r1: Incentivizing reasoning capability in llms
 565 via reinforcement learning. *arXiv preprint arXiv:2501.12948*, 2025.
- 566
- 567 Shibo Hao, Sainbayar Sukhbaatar, DiJia Su, Xian Li, Zhiting Hu, Jason Weston, and Yuandong
 568 Tian. Training large language models to reason in a continuous latent space. *arXiv preprint
 569 arXiv:2412.06769*, 2024a.
- 570
- 571 Shibo Hao, Sainbayar Sukhbaatar, DiJia Su, Xian Li, Zhiting Hu, Jason Weston, and Yuandong
 572 Tian. Training large language models to reason in a continuous latent space, 2024b. URL
 573 <https://arxiv.org/abs/2412.06769>.
- 574
- 575 Alex Havrilla, Yuqing Du, Sharath Chandra Raparthy, Christoforos Nalmpantis, Jane Dwivedi-Yu,
 576 Maksym Zhuravinskyi, Eric Hambro, Sainbayar Sukhbaatar, and Roberta Raileanu. Teaching large
 577 language models to reason with reinforcement learning. *arXiv preprint arXiv:2403.04642*, 2024.
- 578
- 579 David Herel and Tomas Mikolov. Thinking tokens for language modeling. *arXiv preprint
 580 arXiv:2405.08644*, 2024.
- 581
- 582 Sepp Hochreiter and Jürgen Schmidhuber. Long short-term memory. *Neural computation*, 9(8):
 583 1735–1780, 1997.
- 584
- 585 Wesley H Holliday and Matthew Mandelkern. Conditional and modal reasoning in large language
 586 models. *arXiv preprint arXiv:2401.17169*, 2024.
- 587
- 588 Kurt Hornik, Maxwell Stinchcombe, and Halbert White. Multilayer feedforward networks are
 589 universal approximators. *Neural networks*, 2(5):359–366, 1989.
- 590
- 591 Howard Karloff, Siddharth Suri, and Sergei Vassilvitskii. A model of computation for mapreduce.
 592 In *Proceedings of the twenty-first annual ACM-SIAM symposium on Discrete Algorithms*, pp.
 593 938–948. SIAM, 2010.
- 594
- 595 Aviral Kumar, Vincent Zhuang, Rishabh Agarwal, Yi Su, John D Co-Reyes, Avi Singh, Kate Baumli,
 596 Shariq Iqbal, Colton Bishop, Rebecca Roelofs, et al. Training language models to self-correct via
 597 reinforcement learning. *arXiv preprint arXiv:2409.12917*, 2024.
- 598
- 599 Thang Luong and Edward Lockhart. Advanced version of gemini with
 600 deep think officially achieves gold-medal standard at the international math-
 601 ematical olympiad. [https://deepmind.google/discover/blog/
 602 advanced-version-of-gemini-with-deep-think-officially-achieves-gold-medal-standard](https://deepmind.google/discover/blog/advanced-version-of-gemini-with-deep-think-officially-achieves-gold-medal-standard)
 603 jul 2025. Google DeepMind Blog.

- 594 William Merrill and Ashish Sabharwal. The expressive power of transformers with chain of thought.
 595 *arXiv preprint arXiv:2310.07923*, 2023a.
 596
- 597 William Merrill and Ashish Sabharwal. The parallelism tradeoff: Limitations of log-precision
 598 transformers. *Transactions of the Association for Computational Linguistics*, 11:531–545, 2023b.
 599
- 600 William Merrill and Ashish Sabharwal. The expressive power of transformers with chain of thought.
 601 In *The Twelfth International Conference on Learning Representations*, 2024.
 602
- 602 William Merrill, Ashish Sabharwal, and Noah A Smith. Saturated transformers are constant-depth
 603 threshold circuits. *Transactions of the Association for Computational Linguistics*, 10:843–856,
 604 2022.
 605
- 606 William Merrill, Jackson Petty, and Ashish Sabharwal. The illusion of state in state-space models. In
 607 *Proceedings of the 41st International Conference on Machine Learning*, pp. 35492–35506, 2024.
 608
- 608 Philipp Mondorf and Barbara Plank. Liar, liar, logical mire: A benchmark for suppositional reasoning
 609 in large language models. *arXiv preprint arXiv:2406.12546*, 2024.
 610
- 611 Franz Nowak, Anej Svetec, Alexandra Butoi, and Ryan Cotterell. On the representational capacity
 612 of neural language models with chain-of-thought reasoning. In Lun-Wei Ku, Andre Martins,
 613 and Vivek Srikumar (eds.), *Proceedings of the 62nd Annual Meeting of the Association for
 614 Computational Linguistics (Volume 1: Long Papers)*, pp. 12510–12548, Bangkok, Thailand,
 615 August 2024. Association for Computational Linguistics. URL <https://aclanthology.org/2024.acl-long.676>.
 616
- 617 OpenAI. Learning to reason with llms. <https://openai.com/index/learning-to-reason-with-llms/>, 2024. Accessed: 2024-09-23.
 618
- 619 OpenAI. We've scored highly enough to achieve gold at this year's ioi online competition with a
 620 reasoning system — placing #6 when ranked with humans and #1 when ranked with other ais.
 621 in just a few weeks: 2nd at atcoder; gold medal-level at imo; gold medal-level at ioi. <https://x.com/OpenAI/status/1954969035713687975>, aug 2025. Post on X (formerly
 622 Twitter).
 623
- 625 Long Ouyang, Jeffrey Wu, Xu Jiang, Diogo Almeida, Carroll Wainwright, Pamela Mishkin, Chong
 626 Zhang, Sandhini Agarwal, Katarina Slama, Alex Ray, et al. Training language models to follow
 627 instructions with human feedback. *Advances in neural information processing systems*, 35:27730–
 628 27744, 2022.
 629
- 630 Jorge Pérez, Pablo Barceló, and Javier Marinkovic. Attention is turing-complete. *Journal of Machine
 631 Learning Research*, 22(75):1–35, 2021.
 632
- 632 Jacob Pfau, William Merrill, and Samuel R. Bowman. Let's think dot by dot: Hidden computation in
 633 transformer language models. In *First Conference on Language Modeling*, 2024. URL <https://openreview.net/forum?id=NikbrdtYvG>.
 634
- 635 Jack W Rae, Anna Potapenko, Siddhant M Jayakumar, Chloe Hillier, and Timothy P Lillicrap.
 636 Compressive transformers for long-range sequence modelling. *arXiv preprint*, 2019. URL
 637 <https://arxiv.org/abs/1911.05507>.
 638
- 639 Ivan Rodkin, Yurii Kuratov, Aydar Bulatov, and Mikhail Burtsev. Associative recurrent memory
 640 transformer, 2024. URL <https://arxiv.org/abs/2407.04841>.
 641
- 642 Clayton Sanford, Daniel Hsu, and Matus Telgarsky. Transformers, parallel computation, and logarithmic
 643 depth. In *Forty-first International Conference on Machine Learning*, 2024a.
 644
- 645 Clayton Sanford, Daniel J Hsu, and Matus Telgarsky. Representational strengths and limitations of
 646 transformers. *Advances in Neural Information Processing Systems*, 36, 2024b.
 647
- John Schulman, Filip Wolski, Prafulla Dhariwal, Alec Radford, and Oleg Klimov. Proximal policy
 optimization algorithms. *arXiv preprint arXiv:1707.06347*, 2017.

- 648 Zhihong Shao, Peiyi Wang, Qihao Zhu, Runxin Xu, Junxiao Song, Xiao Bi, Haowei Zhang,
 649 Mingchuan Zhang, YK Li, Y Wu, et al. Deepseekmath: Pushing the limits of mathematical
 650 reasoning in open language models. *arXiv preprint arXiv:2402.03300*, 2024.
- 651
- 652 Parshin Shojaee, Iman Mirzadeh, Keivan Alizadeh, Maxwell Horton, Samy Bengio, and Mehrdad
 653 Farajtabar. The illusion of thinking: Understanding the strengths and limitations of reasoning
 654 models via the lens of problem complexity, 2025. URL <https://arxiv.org/abs/2506.06941>.
- 655
- 656 Lena Strobl, William Merrill, Gail Weiss, David Chiang, and Dana Angluin. Transformers as
 657 recognizers of formal languages: A survey on expressivity. *arXiv preprint arXiv:2311.00208*,
 658 2023.
- 659
- 660 Lena Strobl, William Merrill, Gail Weiss, David Chiang, and Dana Angluin. What formal languages
 661 can transformers express? a survey. *Transactions of the Association for Computational Linguistics*,
 662 12:543–561, 2024.
- 663
- 664 Jonathan Uesato, Nate Kushman, Ramana Kumar, Francis Song, Noah Siegel, Lisa Wang, Antonia
 665 Creswell, Geoffrey Irving, and Irina Higgins. Solving math word problems with process-and
 666 outcome-based feedback. *arXiv preprint arXiv:2211.14275*, 2022.
- 667
- 668 Karthik Valmecik, Kaya Stechly, and Subbarao Kambhampati. Llms still can't plan; can lrms? a
 669 preliminary evaluation of openai's o1 on planbench. *arXiv preprint arXiv:2409.13373*, 2024.
- 670
- 671 Ashish Vaswani, Noam Shazeer, Niki Parmar, Jakob Uszkoreit, Llion Jones, Aidan N Gomez,
 672 Łukasz Kaiser, and Illia Polosukhin. Attention is All you Need. In *Advances in neural information
 673 processing systems*, pp. 5998–6008, 2017. URL <http://papers.nips.cc/paper/7181-attention-is-all-you-need.pdf>.
- 674
- 675 Yuxuan Wan, Wenxuan Wang, Yiliu Yang, Youliang Yuan, Jen-tse Huang, Pinjia He, Wenxiang Jiao,
 676 and Michael Lyu. LogicAsker: Evaluating and improving the logical reasoning ability of large
 677 language models. In Yaser Al-Onaizan, Mohit Bansal, and Yun-Nung Chen (eds.), *Proceedings of
 678 the 2024 Conference on Empirical Methods in Natural Language Processing*, pp. 2124–2155, Mi-
 679 ami, Florida, USA, November 2024. Association for Computational Linguistics. doi: 10.18653/v1/2024.emnlp-main.128. URL <https://aclanthology.org/2024.emnlp-main.128>.
- 680
- 681 Peiyi Wang, Lei Li, Zhihong Shao, Runxin Xu, Damai Dai, Yifei Li, Deli Chen, Yu Wu, and Zhifang
 682 Sui. Math-shepherd: Verify and reinforce LLMs step-by-step without human annotations. In
 683 Lun-Wei Ku, Andre Martins, and Vivek Srikumar (eds.), *Proceedings of the 62nd Annual Meeting
 684 of the Association for Computational Linguistics (Volume 1: Long Papers)*, pp. 9426–9439,
 685 Bangkok, Thailand, August 2024. Association for Computational Linguistics. doi: 10.18653/v1/2024.acl-long.510. URL <https://aclanthology.org/2024.acl-long.510>.
- 686
- 687 Jason Wei, Xuezhi Wang, Dale Schuurmans, Maarten Bosma, Fei Xia, Ed Chi, Quoc V Le, Denny
 688 Zhou, et al. Chain-of-thought prompting elicits reasoning in large language models. *Advances in
 689 neural information processing systems*, 35:24824–24837, 2022.
- 690
- 691 Jason Weston, Sumit Chopra, and Antoine Bordes. Memory networks. In Yoshua Bengio and Yann
 692 LeCun (eds.), *3rd International Conference on Learning Representations, ICLR 2015, San Diego,
 693 CA, USA, May 7-9, 2015, Conference Track Proceedings*, 2015. URL <http://arxiv.org/abs/1410.3916>.
- 694
- 695 Liu Yang, Kangwook Lee, Robert Nowak, and Dimitris Papailiopoulos. Looped transformers
 696 are better at learning learning algorithms, 2024. URL <https://arxiv.org/abs/2311.12424>.
- 697
- 698 Shunyu Yao, Dian Yu, Jeffrey Zhao, Izhak Shafran, Tom Griffiths, Yuan Cao, and Karthik Narasimhan.
 699 Tree of thoughts: Deliberate problem solving with large language models. *Advances in Neural
 700 Information Processing Systems*, 36, 2024.
- 701
- Qifan Yu, Zhenyu He, Sijie Li, Xun Zhou, Jun Zhang, Jingjing Xu, and Di He. Enhancing auto-
 702 regressive chain-of-thought through loop-aligned reasoning, 2025. URL <https://arxiv.org/abs/2502.08482>.

- 702 Chulhee Yun, Srinadh Bhojanapalli, Ankit Singh Rawat, Sashank J Reddi, and Sanjiv Kumar.
703 Are transformers universal approximators of sequence-to-sequence functions? *arXiv preprint*
704 *arXiv:1912.10077*, 2019.
- 705 Xiang Zhang, Muhammad Abdul-Mageed, and Laks VS Lakshmanan. Autoregressive+ chain of
706 thought= recurrent: Recurrence’s role in language models’ computability and a revisit of recurrent
707 transformer. *arXiv preprint arXiv:2409.09239*, 2024.
- 709
710
711
712
713
714
715
716
717
718
719
720
721
722
723
724
725
726
727
728
729
730
731
732
733
734
735
736
737
738
739
740
741
742
743
744
745
746
747
748
749
750
751
752
753
754
755

756 A SUMMARY OF MODELS’ PERFORMANCE
757
758

755 **Figure 6: With GRPO as well as with ACT and Orbit-Orbit training depth of reasoning can be**
756 **significantly extended.** Average $DepthScore = 1 + \sum_{i=2}^4 acc(i)$, where $acc(i)$ is the accuracy of
757 predicting the $(10 + i)$ th state based on the first 10 states.

780 B RELATED WORK
781

782 **Computational Expressivity.** Sanford et al. (2024b) show that in setups where the input context
783 length grows but the model depth remains constant, transformers achieve logarithmic complexity
784 scaling in input size for sparse averaging tasks and linear scaling for triple detection. They further use
785 the simulation of transformers in a constant number of MPC (Karloff et al., 2010) communication
786 rounds to demonstrate their expressive power, showing that logarithmic-depth transformers can
787 efficiently solve tasks that are intractable for graph neural networks and recurrent models Sanford
788 et al. (2024a). Merrill & Sabharwal (2023b) prove that transformers with logarithmic precision
789 can be simulated by constant-depth logspace-uniform threshold circuits, implying fundamental
790 computational limitations. Zhang et al. (2024) employ circuit complexity theory to show that
791 bounded-depth transformers cannot directly solve certain arithmetic or equation tasks, unless the
792 model size increases exponentially.

793 **Formal Language Recognition.** The Chomsky hierarchy has been used to classify the computational
794 capabilities of transformers and their expressivity limits. Deletang et al. (2023) show that transformers
795 struggle with non-regular languages. Strobl et al. (2024) provide a comprehensive survey on how
796 transformers relate to formal language classes, identifying the architectural constraints that limit their
797 ability to process hierarchical structures. They show that while transformers with softmax attention
798 can count, they remain within TC^0 and struggle with evaluating Boolean formulas or solving complex
799 hierarchical tasks. Zhang et al. (2024) discuss transformers’ limitations due to their lack of recurrence,
800 arguing that they are computationally weaker than recurrent models in formal language tasks.

801 Several studies explore how CoT enhances transformer reasoning capabilities. Feng et al. (2024) show
802 that transformers can solve arithmetic and dynamic programming tasks via CoT, which they fail to do
803 directly. Merrill & Sabharwal (2024) demonstrate that CoT increases computational power, enabling
804 the recognition of regular languages. Nowak et al. (2024) formalize CoT reasoning probabilistically,
805 showing equivalence to probabilistic Turing machines. Zhang et al. (2024) argue that CoT can
806 approximate recurrent computation, mitigating transformers’ lack of explicit recurrence.

807 There are generalizations of CoT that relax the human-like word-by-word out-loud reasoning. The
808 reasoning process has been moved to special pause (Goyal et al., 2024), think (Herel & Mikolov,
809 2024), or filler (Pfau et al., 2024) tokens to allow the model to think internally before generating
a response. Coconut (Chain of Continuous Thought) Hao et al. (2024a) further extends this by

810 replacing explicit word decoding with the model’s last hidden state as input to the next step, effec-
 811 tively shifting reasoning into the latent space. Moreover, since real-world datasets rarely include
 812 supervision for long, multi-step reasoning, approaches that incorporate verifiers or intermediate
 813 feedback have become increasingly important (Pfau et al., 2024). At the same time, reinforcement
 814 learning methods (Schulman et al., 2017), such as GRPO (Shao et al., 2024), which rely solely on
 815 rewards for correct final answers, show great promise.

816 Overall, these studies highlight the limitations of transformers in reasoning depth and computational
 817 power, showing that CoT-like approaches and recurrence can help mitigate these constraints. Our
 818 work explores the use of One-dimensional Cellular Automata (1dCA) as a framework to evaluate
 819 models’ reasoning abilities. 1dCA provides a flexible and controlled setting where the number of
 820 sequential steps required to solve a task can be precisely defined. Adjusting the complexity of state
 821 transition rules allows for varying task difficulty.

822 **Looped Transformers** Another paper (Yang et al., 2024) investigates whether looped transformers
 823 (Yang et al., 2024) can emulate iterative learning algorithms, such as gradient descent, for data-fitting
 824 problems like linear regression. Their core finding is that looped transformers can achieve comparable
 825 performance to standard transformers with significantly fewer parameters by effectively replicating
 826 these iterative optimization steps. Our paper investigates how different architectures and training
 827 methods affect a model’s ability to learn and perform multi-step reasoning and rule abstraction. The
 828 “iterations” in our study are interpreted as steps for applying a discovered rule or propagating a state,
 829 which is distinct from emulating optimization algorithms.

830 RELAY (Yu et al., 2025) is a framework that aligns CoT steps with loop iterations and uses interme-
 831 diate supervision during looped transformer training to generate high-quality reasoning chains for
 832 auto-regressive models. Their aim is to leverage the length generalization of looped transformers to
 833 improve auto-regressive models’ handling of longer reasoning chains. In our paper, we study CoT as
 834 a training objective that provides direct reasoning supervision on intermediate states for multi-step
 835 state prediction on 1dCA. While both studies involve recurrence and CoT-like supervision, Yu et
 836 al.’s work focuses on a specific methodology for generating CoT for other models by aligning CoT
 837 steps with loops, whereas our work directly evaluates how training with or without intermediate
 838 supervision, as in O-O or GRPO, respectively, influences a model’s core reasoning capabilities in a
 839 disentangled environment.

840 In the “Illusion of Thinking” research (Shojaee et al., 2025) authors show that the models’ performance
 841 decreases with the increased complexity of puzzle environments. For thinking models, however, this
 842 degradation is less dramatic. Which is consistent with our findings on Figure 5 (A).

843 C MODELS DISCUSSION

844 **LSTM** By integrating a gating mechanism into recurrent neural networks, LSTMs alleviated
 845 the vanishing gradient problem, allowing the model to retain information from up to 10–15 prior
 846 time steps. However, LSTMs still face several limitations. First, despite the gating mechanism,
 847 they often struggle with very long-range dependencies, as information can decay over extended
 848 sequences. Second, their sequential nature hinders parallelization, which slows training and increases
 849 computational cost compared to more modern architectures such as transformers. As a result, while
 850 LSTMs represented a major breakthrough in sequence modeling and in theory can process contexts
 851 of infinite length, they have been largely superseded by more scalable and efficient models.

852 **Transformers** Attention mechanism allows transformers to dynamically focus on relevant parts
 853 of the input, facilitating effective information integration across long distances. As a result, they
 854 maintain and reuse context more effectively than LSTMs, making them a powerful backbone for
 855 modern large language models. This design has enabled state-of-the-art performance on complex
 856 reasoning tasks, cementing the transformer’s role at the forefront of natural language processing.

857 While this flexibility is powerful, it also introduces drawbacks. Transformers must compute and
 858 store a large attention matrix, often scaling to $O(n^2)$ in both memory and computation. This creates
 859 challenges when handling very long inputs or generating lengthy outputs, as hardware and software
 860 limitations cap the practical context window. Another limitation of transformers is their difficulty
 861 in processing information “in-depth.” Each generation step requires a fixed amount of computation,

864	Model	Depth	d_{model}	$d_{\text{mem}} / \text{state_size}$	n_{heads}	max ACT iterations
865	GPTNeox	4	128	-	4	4
866	ARMT	4	128	32	4	4
867	Mamba	4	128	16	-	4
868	LSTM	4	128	-	-	4

869
870 Table 1: **Hyperparameters for the base models.** We used these hyperparameters in the O-S, O-O,
871 O-RS and RO-S experiments, as well as CoT and GRPO experiments.
872

873 constrained by the number of transformer layers. Consequently, transformers face challenges with
874 multi-hop reasoning. To enable more efficient in-depth reasoning, various test-time compute strategies
875 have been introduced, including chain-of-thought prompting, Monte Carlo Tree Search, and others.
876 While these techniques partially mitigate the issue, they remain bottlenecks: longer generations
877 demand substantial computational resources and may exceed the effective context window. These
878 techniques also require supervision for intermediate steps to train the model. This is a huge limitation
879 as strong AGI systems should automatically learn to recursively apply rules to data.
880

881 **State Space Models** While less prevalent compared to RNNs and transformers, SSMs are widely
882 used in control theory and signal processing. In the context of neural networks, SSMs aim to combine
883 the strengths of recurrent models, such as handling infinitely large contexts, with the efficiency of
884 convolutional models for fast prompt processing and training. This positions SSMs as a middle
885 ground between classical LSTMs and transformers.
886

887 In our experiments, we utilize Mamba, an SSM variant improved with a selective mechanism (Gu &
888 Dao, 2023; Gu et al., 2021). The Mamba Selective State Model extends this framework by making A ,
889 B , and C dynamic, adjusting them based on the input $x(t)$. This adaptive mechanism allows Mamba
890 to selectively focus on relevant input features, filtering out irrelevant details (Gu & Dao, 2023). By
891 dynamically adapting its parameters, Mamba is able to capture long-range dependencies in sequences
892 while remaining computationally efficient.
893

894 While SSMs excel in efficiently modeling long-range dependencies and processing sequential data
895 with reduced computational overhead compared to transformers, they typically lack the expressiveness
896 and flexibility required for advanced reasoning tasks. These models may face challenges in capturing
897 complex, hierarchical relationships, compounding the limitations already present in transformers
898 when it comes to in-depth reasoning.
899

900 **Associative Recurrent Memory Transformer** As shown in Rodkin et al. (2024), ARMT can
901 leverage information from the distant past of up to 50 million tokens. Compared to SSMs, ARMT is
902 more expressive due to its grounding in the classical transformer architecture, while it also introduces
903 the ability to recurrently process contexts of infinite length.
904

905 **Theoretical Depth Estimates** Theoretical estimates predict that for GPTNeox and Mamba depth
906 of computation is limited by the number of layers $Depth = O(L)$, where L is the number of model
907 layers. For LSTM computational depth not only grows with the number of layers, but also with the
908 sequence length, making $Depth = O(L + N)$, here N is the sequence length. ARMT is a trade-off
909 between parallelization and recurrence. It utilizes the forward transformer for local processing of
910 the segment, but passes its recurrent state between segments in RNN-like format, which allows its
911 computational depth to grow with the sequence length, making $Depth = O(L + \frac{N}{S})$, here S is the
912 segment size.
913

D TRAINING DETAILS

914 We train all our models for 40k steps with Adam optimizer with learning rate 3e-4 with linear warmup
915 for 1000 steps and linear decay. We use total batch size of 256 samples. The vast majority of
916 experiments we ran on single NVIDIA RTX 6000 Ada GPU. Models hyperparameters can be found
917 in Table 1.
918

918 E ADAPTIVE COMPUTATION TIME FORMULATION
919920 The module calculates a halting weight p_t at each computation step t , which represents the percentage
921 of the task completed by the module f :
922

923
$$p_t = \text{HALT}(h_t); \quad h_{t+1} = f(h_t), \quad \text{HALT}(h_t) = \sigma(W_h h_t + b_h) \quad (1)$$

924

925 where h_t is the layer input. This weight is accumulated into P_t until the halting condition is met:
926

927
$$P_t = \sum_{i=0}^t p_i; \quad T = \text{argmin}_t (P_t \geq 1 - \epsilon) + 1. \quad (2)$$

928

929 Finally, the prediction is done in the following way: $y = \sum_{t=0}^{T-1} p_t h_{t+1}$ with $p_{T-1} = R =$
930 $1 - \sum_{t=0}^{T-2} p_t$. For training, we add an auxiliary component to the loss function $\hat{L} = L + \tau R$. This
931 component serves as a time penalty.
932933 F SAMPLES EXAMPLES
934

935 F.1 HANDSUP GAME

936 You peek through a doorway into a cosy room.
937 7 friends sit around a round table in this order: Alice, Bob, Carol,
938 Dave, Erin, Frank, and Grace - and then back to Alice again.
939 They don't talk. At the end of each round they all decide, at the very
940 same moment, either to raise a hand or to keep both hands on the table.
941
942 You watch and jot down what happens:
943 - Round 1. Alice, Bob, Dave, Erin, Frank, and Grace raise their hands.
944 The others keep their hands on the table.- Round 2. Alice, Carol,
945 Erin, Frank, and Grace raise their hands. The others keep their hands
946 on the table.- Round 3. Bob, Dave, Frank, and Grace raise their
947 hands. The others keep their hands on the table.- Round 4. Alice,
948 Carol, and Erin raise their hands. The others keep their hands on the
949 table.- Round 5. Bob and Dave raise their hands. The others keep
950 their hands on the table.
951 Now it's your turn to be the clever observer.
952 Puzzle: What will each friend do in Round 6?
953 Please answer in plain words, going in order around the table, starting
954 from the first name above. Answer with the list of people with hands
955 up, not mentioning the ones with hands down. For example: Alice, Bob,
956 and Dave raise their hands.

957 F.2 ECA - R2S20T10
958959 The samples from our open dataset.
960961 The input vocabulary of the tested models consists of the following tokens: [0], [1], and [SEP].
962 The states and the local rule ρ are encoded as binary strings. The model receives the orbit as a
963 sequence of bits, representing consecutive states separated by the [SEP] tokens.
964965 We train the model to predict the blue tokens.
966967 In all these examples rule is 0101111100100000101111011111100 and the initial state is
968 10110111001000110100.
969970 **O-S**
971972 10110111001000110100<sep>1110100110111101100<sep>10111011010000111011<sep>
973 11001110111011101100<sep>10111011001100111011<sep>11001110111011101100<sep>
974 10111011001100111011<sep>11001110111011101100<sep>10111011001100111011<sep>
975 11001110111011101100<gen>**10111011001100111011**976 **O-O**

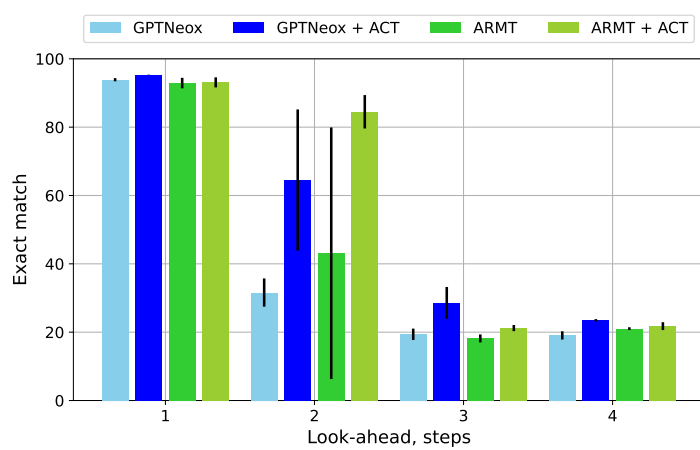


Figure 7: **ACT outperforms the base model on multiple prediction horizons task.** Exact match accuracy (mean \pm std) for cellular automata state prediction across different look-ahead horizons. Models receive initial 10 states followed by a special shift token (1-4) indicating prediction horizon.

10110111001000110100<sep>1110100110111101100<sep>10111011010000111011<sep>
 1100111011101101100<sep>10111011001100111011<sep>11001110111011101100<sep>
 10111011001100111011<sep>11001110111011101100<sep>10111011001100111011<sep>
 11001110111011101100<gen>**10111011001100111011<sep>11001110111011101100<sep>**
10111011001100111011<sep>11001110111011101100

O-RS

10110111001000110100<sep>1110100110111101100<sep>10111011010000111011<sep>
 11001110111011101100<sep>10111011001100111011<sep>11001110111011101100<sep>
 10111011001100111011<sep>11001110111011101100<sep>10111011001100111011<sep>
 11001110111011101100<gen>**010111110010000010111101111100<sep>**
10111011001100111011

RO-S

01011111001000001011101111100<sep>10110111001000110100<sep>
 1110100110111101100<sep>10111011010000111011<sep>11001110111011101100<sep>
 10111011001100111011<sep>11001110111011101100<sep>10111011001100111011<sep>
 11001110111011101100<sep>10111011001100111011<sep>11001110111011101100<gen>
10111011001100111011

G MULTIPLE PREDICTION HORIZONS TRAINING

Given an orbit $\mathcal{O}^T(x)$ and the random shift token $s_i \in \{s_1, s_2, s_3, s_4\}$ the objective is to predict the state $x^{(T+i-1)}$. In this setup, we train the model to reason more for some inputs than others.

We conducted experiments where a single model was trained to handle multiple prediction horizons (1-4 steps ahead) using special shift tokens in the input format: `[x_0] [SEP] ... [x_9] [shift_k] [gen] [MASK]` where $k \in \{1, 2, 3, 4\}$ indicates the required look-ahead. As shown in Figure 7, baseline GPTNeox performs 32% shift=2 and 19% for shift=4. Introducing ACT substantially mitigates these drops.

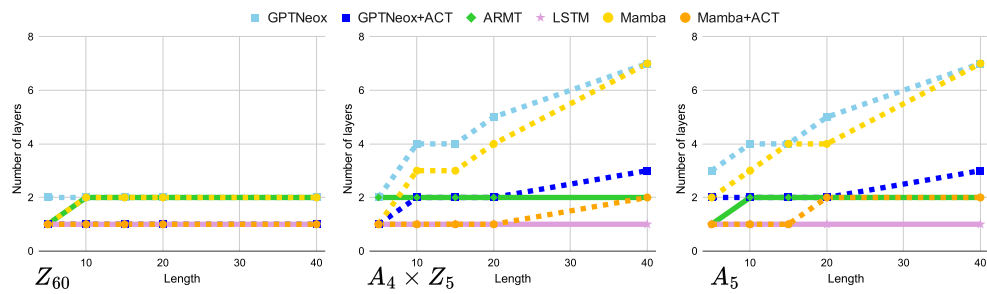
The ARMT architecture shows comparable characteristics – while baseline performance at shift=2 is stronger than GPTNeox (43% vs 32%), ACT provides similar absolute improvements (85% at shift=2). However, both architectures exhibit similar limitations at the longest horizons (shift=4), with all variants scoring 21%-25%, indicating challenges in extreme-depth reasoning.

1026 H GROUP MULTIPLICATION TASK

1028 The task is, given the sequence of elements of some group, label each element with the product of
 1029 all previous elements of the sequence, including the current one. This task is relevant to reasoning
 1030 because it provides a controlled setup with tasks of different computational complexity.

1031 We evaluated our models in 3 groups of different difficulty: Z_{60} , $A_4 \times Z_5$, and A_5 ; and different
 1032 sequence lengths: 5, 10, 15, 20, and 40. For each model, we report the minimal number of layers
 1033 to achieve 70% exact match accuracy. For the sake of consistency with previous works, we slightly
 1034 changed the hyperparameters of our models. We use $d_{\text{model}} = 512$ and $n_{\text{heads}} = 8$. For the ARMT
 1035 model, we use the segments of size 2.

1036 As shown in Figure 8, the required depth for solving longer tasks grows for GPTNeox and Mamba
 1037 models, while staying constant (1-2 layers) for the models with recurrence (ARMT and LSTM). More-
 1038 over, depth requirements can be significantly reduced by adding Adaptive Computation Time (ACT)
 1039 or Associative Memory (ARMT), which is consistent with our findings on the 1dCA benchmark.
 1040 LSTM, however, performs much better, being able to solve the problem with just one layer.



1052 **Figure 8: ACT significantly reduces the required models’ depth for the majority of group**
 1053 **multiplication tasks.** Each chart contains the information about the minimal required number of
 1054 layers for solving task of given length with 70% exact match accuracy. GPTNeox and Mamba being
 1055 TC^0 -limited models require more layers for solving deeper (longer in this case) tasks, while ARMT
 1056 and LSTM solve them with constant number of layers.

1058 I ABLATION STUDIES

1061 Originally, ACT was applied to single-layer NNs (Dehghani et al., 2019; Graves, 2016). When it
 1062 comes to deep models, we can apply ACT to each layer of the model, averaging the remainders
 1063 over the layers to add as the time penalty to the loss (layer-wise ACT or LACT). Another option is
 1064 to apply ACT to the whole backbone model (MACT), which maps the $\mathbb{R}^{N \times d} \rightarrow \mathbb{R}^{N \times d}$ (therefore
 1065 without embedding and unembedding layer). In our ablation studies, we compare layer-wise ACT
 1066 and model ACT but find that they perform similarly. See I.2 for more details. Therefore, in the main
 1067 experiments, we use only layer-wise ACT and always refer to this version.

1068 To determine whether performance gains stem from the adaptive nature of computation time or merely
 1069 from increased computation, we include a fixed computation time (FCT) baseline in our ablation
 1070 study (I.1). Specifically, we examine the case of three fixed iterations, chosen to match the upper
 1071 bound of the average number of ACT operations observed in our experiments.

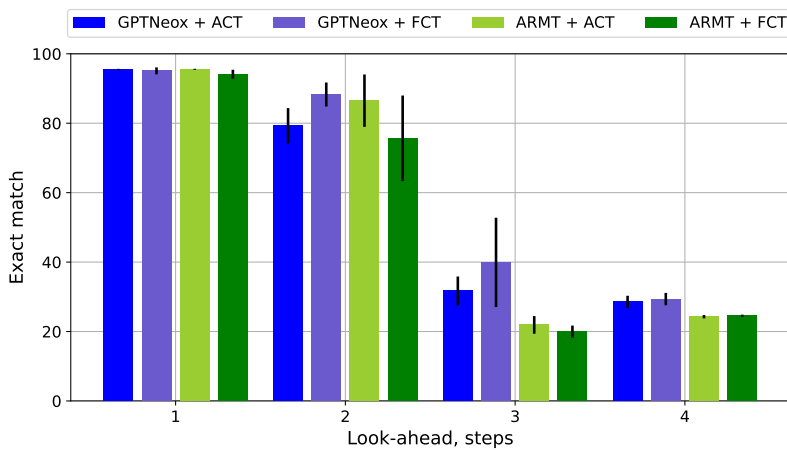
1072 Here, we present several auxiliary studies of various ACT variants.

1074 I.1 FIXED NUMBER OF STEPS IN ACT VS DYNAMIC NUMBER OF STEPS

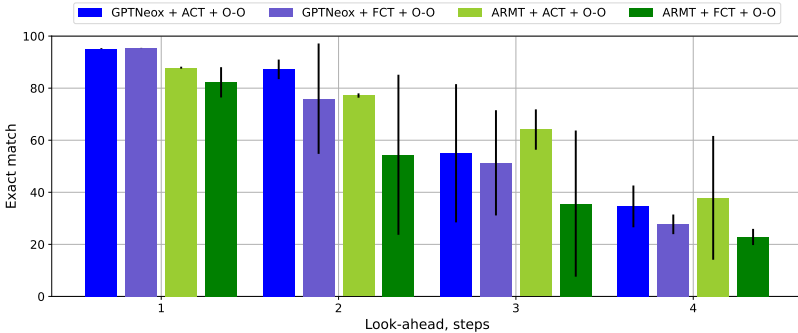
1076 We conduct experiments with a fixed number of steps to assess the need for adaptivity in computation
 1077 time. A constant depth of 3 was selected based on experiments with ACT, which demonstrated that
 1078 this represents the upper limit of the number of steps reached for any hidden state. The results with
 1079 Fixed Computation Time (FCT) and ACT as the baseline are presented in Figure 9 and Figure 10 for
 O-S and O-O settings respectively.

1080 In O-S setting, FCT improved the exact match in look-ahead 2, 3 for GPTNeox, but performed worse
 1081 in look-ahead 2 for ARMT. In contrast, in the O-O setting, FCT showed reduced performance for
 1082 both GPTNeox and ARMT in look-ahead 2, 3, 4.

1083 Therefore, adaptivity in computation time might find the optimal amount of steps leading to enhanced
 1084 exact match, or perform equivalently with fewer steps.



1102 **Figure 9: Fixed Computation Time (FCT) with 3 iteration steps performs on par with Adaptive
 1103 Computation Time (ACT) in Orbit-State task.** Exact match accuracy (mean \pm std) for cellular
 1104 automata state prediction across different look-ahead horizons.



1118 **Figure 10: Fixed Computation Time (FCT) with 3 iteration steps underperforms Adaptive
 1119 Computation Time (ACT) in Orbit-Orbit task.** Exact match accuracy (mean \pm std) for cellular
 1120 automata state prediction across different look-ahead horizons.

I.2 MODEL-ACT vs LAYER-ACT

1124 Figure 11 shows that Layer-ACT performs similarly or better compared to Model-ACT. In particular,
 1125 Model-ACT has a similar processing pattern to the COCONUT model (Hao et al., 2024b), passing
 1126 the hidden states from the model output to the input. Therefore, a similar reasoning behavior is
 1127 expected. A notable difference is observed when these types of ACT are applied to ARMT. However,
 1128 it is important to note that training was stopped after 30,000 steps, and the model with MACT
 1129 augmentation did not have sufficient time to fully converge. All models in this experiment adhered to
 1130 these training restrictions to ensure a fair comparison.

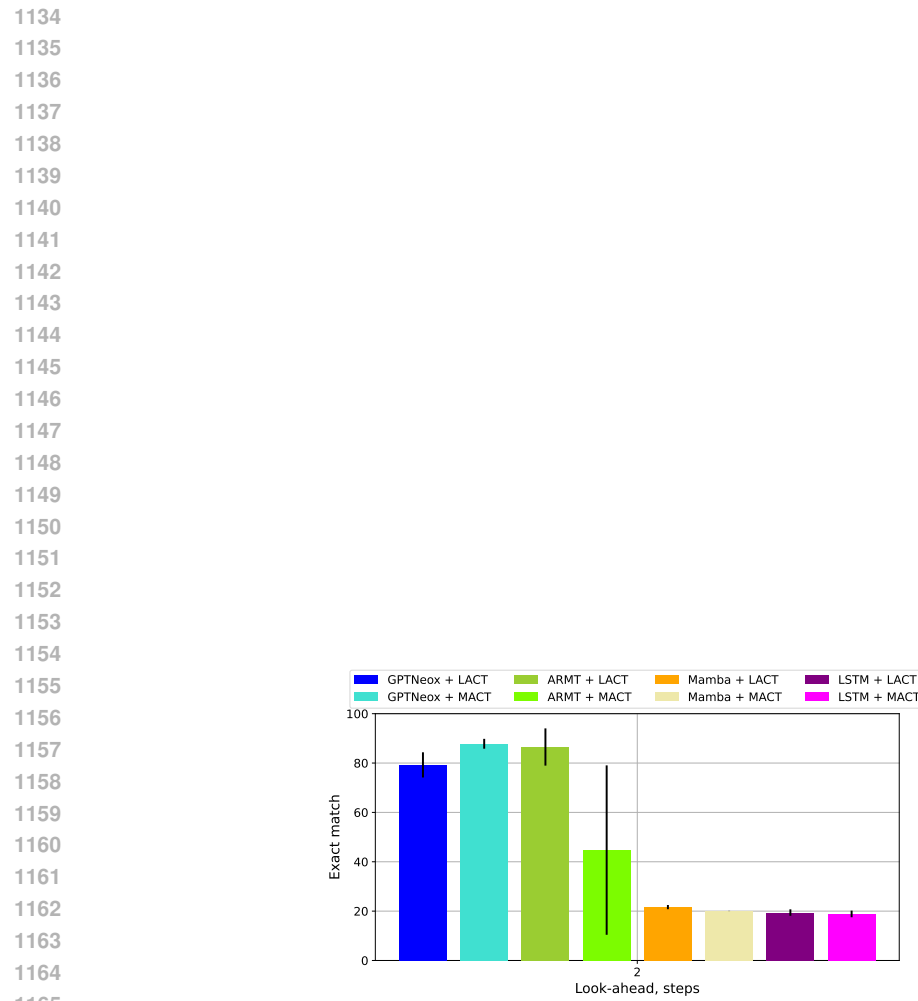


Figure 11: Layer-ACT performs similar or better compared to Model-ACT. Exact match on cellular automata state prediction task with look ahead 2.